Electrodeposition of Cu$_2$O: An Excellent Method for Obtaining Films of Controlled Morphology and Good Performance in Li-Ion Batteries

J. Morales,[a,*] **L. Sánchez,**[a,z] **S. Bijani,**[b] **L. Martínez,**[b] **M. Gabás,**[b] **and J. R. Ramos-Barrado**[b,*]

aDepartamento de Química Inorgánica e Ingeniería Química, Campus de Rabanales, Universidad de Córdoba, 14071 Córdoba, Spain
bDepartamento de Física Aplicada I, Laboratorio de Materiales y Superficies, Campus de Teatinos, Universidad de Málaga, 29071 Málaga, Spain

Highly uniform films of pure electrodeposited Cu$_2$O in variable particle size (micronic and submicronic), morphology, and thickness (0.3-13 μm) depending on the applied potential and the amount of electrical charge transferred were examined as working electrodes in lithium cells to check their suitability as anodes for Li-ion cells. The thinnest film studied delivered a specific capacity close to the theoretical value; such a capacity decreased with increasing film thickness and particle size. All films except the thickest exhibited excellent capacity retention upon extensive cycling irrespective of particle size. On similar thickness, the discharge capacity increased with decreasing particle size.
© 2005 The Electrochemical Society. [DOI: 10.1149/1.1854126] All rights reserved.

Oxides of 3d transition metals (Fe, Co, Ni, and Cu) react reversibly with lithium in a lithium cell below 1.5 V.[1] As shown by a number of studies, such a singular property makes them potential candidates for use as negative electrodes in Li-ion batteries.[2-5] Copper oxides perform especially well in lithium cells;[6] also, they are nontoxic, abundant and hence inexpensive. However, most studies in this context have focused on bulk materials and few have dealt with the performance of these oxides in thin film electrodes.[7,8] The increasing interest aroused by thin Li-ion batteries for potential applications such as smart cards, CMOS-based integrated circuits and microdevices has opened up promising prospects for these novel material-based electrodes. Recently, our group reported on the electrochemical performance of nanocrystalline CuO thin films prepared by spray pyrolyis deposition from copper acetate solutions.[9] These electrodes exhibit a good electrochemical response in lithium cells. However, this preparation methodology is confronted with a serious drawback (*viz.* the difficulty of obtaining clean surface deposits).

Electrochemical deposition is one of the most attractive methods for the synthesis of thin films. It provides advantages such as the ability to use a low synthesis temperature, low costs, and a high purity in the products. Also, electrodeposition allows the stoichiometry, thickness, and microstructure of the films to be controlled by adjusting the deposition parameters. A variety of materials can be prepared in this way.[10,11] The usefulness of this method for designing electrodes for lithium batteries is also well-documented, particularly for tin alloy-based materials.[12,13] In this work, the electrochemical deposition method was used to prepare Cu$_2$O films, which were recently shown to react reversibly with Li.[14] Because the composition and microstructure of the films thus obtained is strongly affected by deposition variables, the primary aim of this work was to explore the possibility of obtaining Cu$_2$O films of variable morphology over the same substrate simply by adjusting the deposition parameters. The structural and textural properties of the films were determined from X-ray diffraction (XRD), X-ray photoelectron spectroscopy (XPS), and scanning electron microscopy (SEM) measurements; also, their reactivity towards Li in lithium cells was tested. The films were found to exhibit excellent capacity retention upon extended cycling.

Experimental

Cu$_2$O electrodeposition was accomplished by using a conventional three-electrode single-compartment electrochemical cell.

Cu$_2$O films were electrodeposited in the potentiostatic mode on titanium substrates (plates 1 cm^2 in surface area) that were previously polished with emery paper, rinsed with deionized water, immersed in 24% HF for 20 s, and rinsed with water. A platinum sheet was used as counter-electrode and saturated calomel electrode (SCE) as reference electrode. Cu$_2$O was electrodeposited by reduction of an alkaline aqueous solution of cupric lactate according to the reaction $2Cu^{2+} + 2e^- + 2OH^- \rightarrow Cu_2O + H_2O$, which was previously reported by Zhou and Switzer.[15] The electrolytic bath contained copper (II) sulphate (0.4 M), and 3 M lactic acid as chelating agent; its pH was adjusted to 9 with sodium hydroxide. The bath temperature was 30°C. Variable applied potentials were tested with a view to obtain Cu$_2$O films of diverse microstructure and morphology. Deposits were air-dried at 100°C for further characterization.

Films were deposited by using an AMEL 2053 potentiostat. The structure and phase composition of the electrochemically deposited films were identified by X-ray diffraction (XRD) on a Siemens D5000 diffractometer using Cu Kα radiation. The chemical composition of the films was examined by XPS. Spectra were recorded on a Physical Electronics PHI 5700 spectrometer using nonmonochromated Mg Kα radiation ($h\nu$ = 1253.6 eV). Binding energies were corrected with the binding energy values for C(1s) of adventitious carbon fixed at 284.6 eV. Spectra were processed by using PHI-Access V.6 and Multipak software, both from Physical Electronics. High-resolution spectra were fitted after Shirley background correction and satellite subtraction. The surface morphology of the films was examined in a JEOL JSM-5410 SEM.

Electrochemical measurements were made in a two-electrode cell, using lithium as counter-electrode. The electrolyte used was Merck battery electrolyte LP 40, which consists of 1 M LiPF$_6$ in ethylene carbonate (EC) and dimethyl carbonate (DEC) in a 1:1 w/w ratio. Rectangular 8 × 9 mm pieces of titanium coated with the active material were used as working electrodes. The amount of oxide attached to the substrate was determined by weighing the substrate before and after electrodeposition on a Sartorius microbalance sensitive to within ±1 μg. Cells were galvanostatically charged and discharged at a C/12 cycling rate, C being defined as 1 Li$^+$ exchanged in 1 h. All electrochemical measurements were controlled via a MacPile II potentiostat-galvanostat.

Results and Discussion

The electrodeposition potential required for a synthesis in the potentiostatic mode is usually unknown. In this situation, linear sweep voltammetric measurements help one identify oxidation-reduction processes potentially undergone by the system of interest

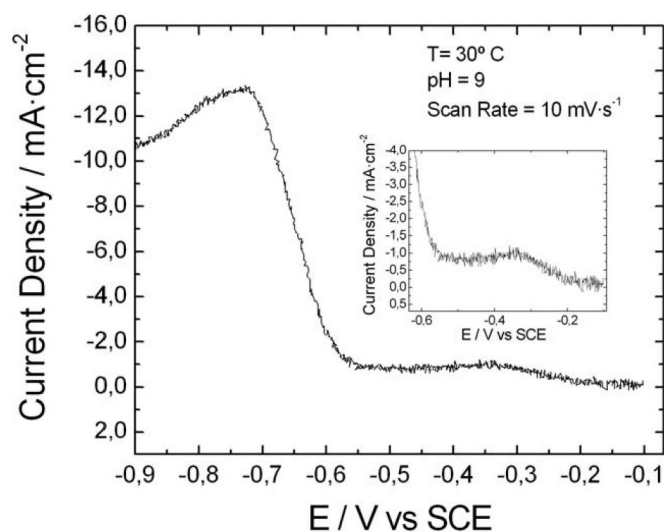* Electrochemical Society Active Member.
z E-mail: luis-sanchez@uco.es

Figure 1. Linear sweep voltammogram for an aqueous solution of Cu^{2+}.

Figure 2. XRD patterns for Cu_2O films electrochemically deposited under different experimental conditions. Ti peaks are marked with an asterisk.

and choose an appropriate potential. Figure 1 shows a typical cathodic scan performed between -100 and -900 mV at a scan rate of 10 mV·s^{-1}. The peak at -350 mV corresponds to the reduction of Cu^{2+} to Cu^+ and the subsequent formation of Cu_2O. On the other hand, the peak at *ca.* -700 mV is due to the reduction of Cu_2O to Cu. Therefore, the potential for the formation of stable Cu_2O ranges from -150 to -600 mV. Once the deposition conditions were established, Cu_2O films of variable morphology were obtained by changing the electrodeposition potential. Of the many deposits obtained, we selected five (Samples A, B, C, D, and E) the deposition conditions, amount deposited and coating thickness of which are shown in Table I.

The XRD patterns obtained over the applied potential range -150 to -575 mV (Fig. 2) exhibited the Ti peaks for the substrate, but none suggesting the presence of phases other than Cu_2O. The amount of material deposited, and hence that of electrical charge transferred, had no influence on film composition, only on peak intensity. No preferred orientation was detected, the relative intensities of diffracted lines were consistent with those tabulated in the corresponding JCPDS card. However, the potential used affected X-ray line broadening, which suggests differences in the degree of crystallinity between films. The signal-to-noise ratio was much better for the films deposited at the less negative potentials and diffraction peaks were appreciably broader for the films deposited at an applied potential of -575 mV. The full width at half-maximum (fwhm) for the two strongest reflections are shown in Table I. The lower crystallinity of Samples C, D, and E precluded accurate evaluation of the width of the (200) peak.

The morphology the films deposited at an applied potential of -150 mV was similar to that reported by Laik *et al.*[14] and Zhou and
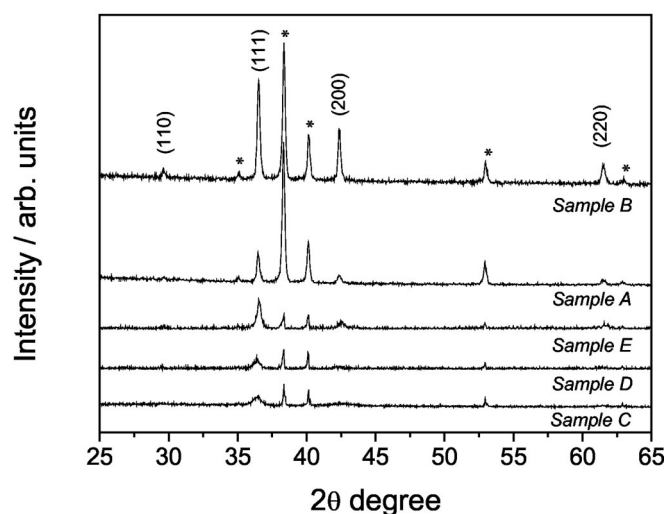
Switzer,[15] namely: regular, well-faceted, polyhedral crystallites (Fig. 3a) the agglomeration degree of which increased with increasing deposition time. The length of the largest polyhedral edges ranged from 1 to 2 μm. By contrast, the films deposited at the more negative potentials (-575 mV) exhibited a granular morphology and the grain agglomerates a cauliflower-like appearance (Fig. 3b) irrespective of the deposition time used, and hence of the film thickness. It should be noted that the grains were always smaller than 1 μm (*ca.* 150-300 nm). Thus, the SEMs revealed that particle morphology and size in the films deposited at an applied potential of -575 mV were rather different from those of the films deposited at -150 mV. This is consistent with the XRD patterns, where the films deposited at the more negative potential exhibited broader diffraction peaks. The electrochemical performance tests of Cu_2O film electrodes were conducted on these two groups of samples on account of their highly disparate morphologies.
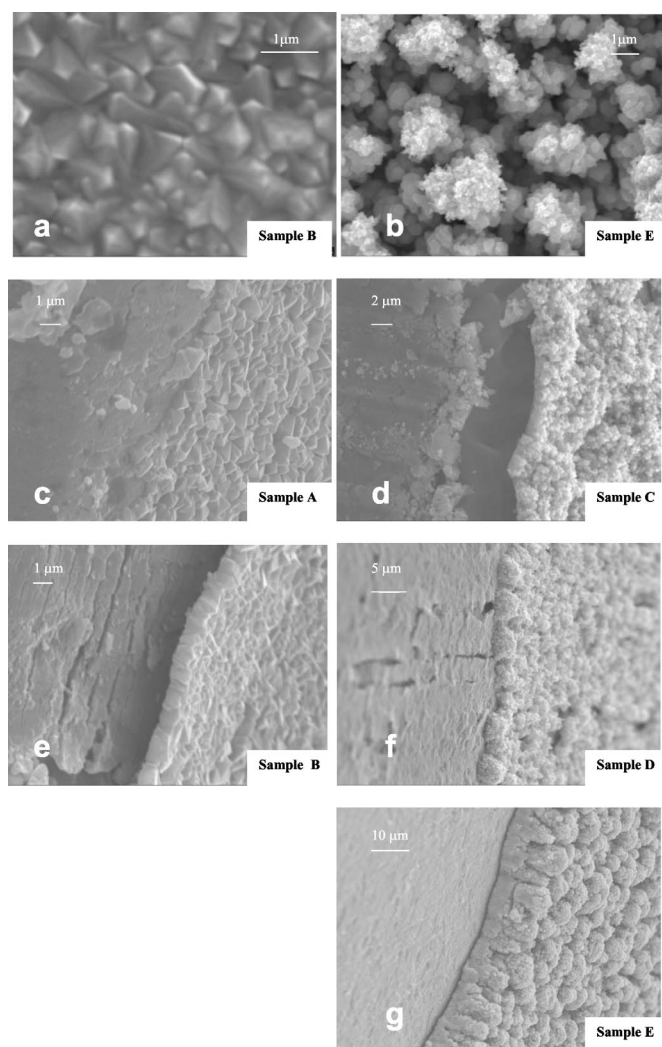
The chemical composition of the films was studied from XPS measurements by varying the emission angle to shift the effective electron escape depth.[16] Alternative methods for assessing changes in oxygen stoichiometry such as those based on the variation of the concentration with depth proved unsuitable for these films owing to the ease with which Cu^{n+} is reduced by Ar^+ bombardment.[17] Figure 4 shows the Cu 2p XPS spectra for sample E as recorded with the analyzer at an angle of 15°, 45°, and 75°, which correspond to different depths in the film. All spectra were identical, with an fwhm of 1.35 eV for the $Cu2p_{3/2}$ peak; this testifies to the high homogeneity of the films. The absence of "shake up" satellites excludes the presence of Cu^{2+} and the binding energy for Cu $2p_{3/2}$, 932.7 eV, together with the modified Auger parameter, 1849.5 eV, indicate that the sole oxidation state in these deposits is Cu^+.[18] This is clearly

Table I. Preparation conditions and selected properties of Cu_2O thin films.

Film	Potential (V)	Electrical charge transfer (C)	Mass deposited (mg cm^{-2})	Thickness[a] (μm)	fwhm[b] (111)	fwhm[b] (200)
Sample A	-150	0.53	0.18	0.3	0.2	0.3
Sample B	-150	1.68	0.6	1.1	0.2	0.2
Sample C	-575	1.00	0.92	1.3	0.6	-
Sample D	-575	2.68	1.19	3.5	0.5	-
Sample E	-575	10.11	4.6	13.3	0.4	-

[a] Values estimated from SEM images.
[b] Angle 2θ.

Figure 3. SEM images for Cu₂O deposits. (a) and (b) Top view c-g cross-sectional view.


Figure 4. High-resolution XPS spectra for Cu 2p corresponding to sample E as recorded at different angles between the analyzer and the film surface. 15° (○); 45° (×); and 75° (●).

consistent with the XRD results, from which a single, Cu₂O crystalline phase can be inferred. No other signals for the substrate or other atoms potentially involved in the electrodeposition process such as sodium or sulphur were detected. Only adventitious C, the presence of which was mainly due to specimen handling and the signal for which disappeared after few seconds of Ar⁺ etching, was detected. Therefore, our films possess a clean surface in addittion to high homogeneity and purity.

Figure 5 shows the first galvanostatic discharge-charge curves for Li/Cu₂O cells. The discharge curves for Samples A and B (Fig. 5a) are similar and exhibit an abrupt drop in potential up to 1.25 V, followed by a smooth decrease up to 0.7 V. The Faradaic yield at such a potential is consistent with the following reaction

$$Cu_2O + 2e^- + 2Li^+ \rightarrow 2Cu + Li_2O \qquad [1]$$

Below 0.7 V, the potential drop was more pronounced; an additional capacity of *ca.* 1 Li⁺ per formula unit was obtained at 0.0 V. This is only one-third of the value reported by Laik *et al.*[14] for electrodeposited Cu₂O of similar particle morphology and has been ascribed to reduction of the electrolyte. It is likely that the Swagelok-type cell used in this work was the origin of the discrepancy as the amount of electrolyte was smaller than that employed in Ref. 14, an electrochemical quartz crystal microbalance. The discharge profiles for Samples C, D, and especially, E, are rather dif-

ferent (Fig. 5b). For samples C and D, the lithium uptake up to 0.7 V was *ca.* 1.7 per formula unit; for Sample E, it was barely 0.4. By contrast, the additional capacity of this latter sample was equivalent to the uptake of 1 Li per formula unit, which is similar to that for Sample A. Of the two main differences between the deposits (*viz.* particle morphology and film thickness), the latter seems to be the more influential. Cu₂O is known to be a poor semiconductor. Thus, an increased thickness, and hence an increased amount of material deposited, restricts the mobility of charge carriers, the cell becoming strongly polarized as a result. One must bear in mind the absence of conducting additives such as carbon black from these electrodes. Thus, in Sample E (*viz.* that with thickest film), Reaction 1 took place to a very small extent and most of the current was used to reduce the electrolyte. The absence of a slope change between 2.5 and 2.0 V, ascribed to CuO reduction,[9,19] is consistent with the XRD and XPS data and excludes the presence of impurities of divalent copper.

The charge curves exhibited strong polarization the intensity of which was also dependent on film thickness. At best, the cell made from Sample A removed about 1.5 Li⁺ ions per formula unit at a cut-off voltage of 3.0 V, which is below the theoretical value for the Cu → Cu₂O oxidation process. However, the removal of up to 2 Li⁺ has been reported for electrodeposited Cu₂O.[14] Theoretical calculations provided a film thickness of 210 nm, which is smaller than those in Table I. These results confirm the prominent role of layer thickness in the electrochemical response of these films. This was further confirmed for Sample E, which scraped from the substrate and the resulting powder mixed with polytetrafluoroethylene (PTFE) (5 wt %), and acetylene black (10 wt %). The electrode was prepared by pressing the active material in an stainless steel grid. The corresponding discharge and charge curves, not shown here, exhibited a different capacity. Thus, 2.0 faraday·mol⁻¹ was calculated for the oxidation process, consistent with a completely reversible character for Reaction 1.

Figure 5c shows the electrochemical response of the different samples on cycling over the 3.0-0.0 V range. Four of the five electrodes successfully preserved the capacity values delivered at the initial stages over 100 cycles. The best performing cell was that made from sample A. Its initial capacity, 275 Ah·kg⁻¹, slowly increased over the first ten cycles and then to a mean value of *ca.* 350 Ah·kg⁻¹, close to the theroretical one for Reaction 1 (375 Ah·kg⁻¹)
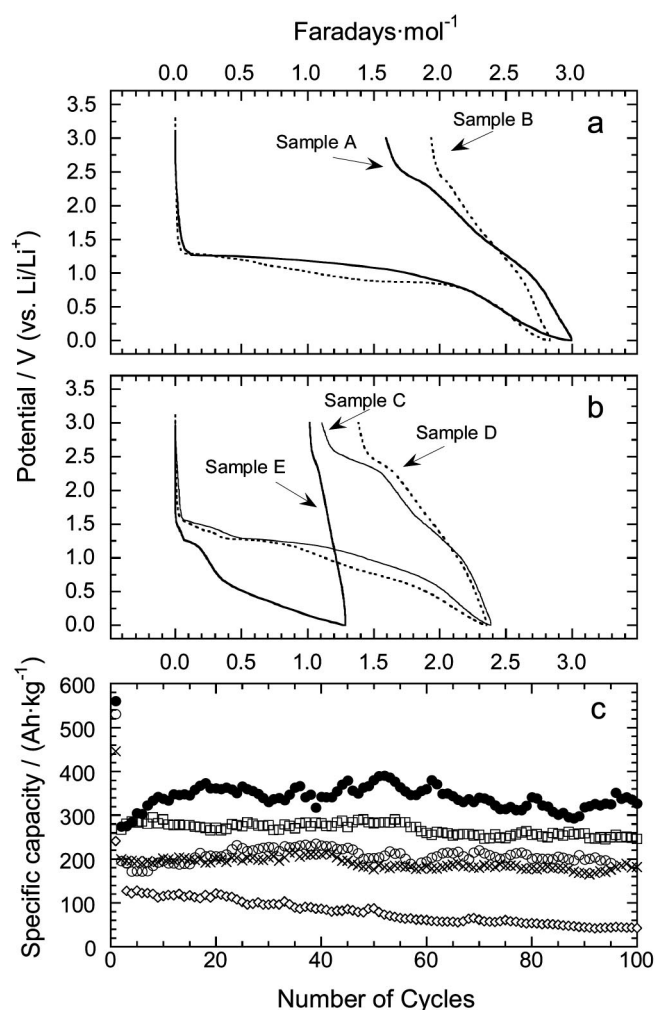
Figure 5. First discharge-charge curves (a and b) and cycling properties for Cu_2O deposits (c) [Sample A (●), Sample B (○), Sample C (□), Sample D (×), Sample E (◇),].

over the next 90. The increase in electrochemical activity of the film over the first few cycles suggests the progressive participation of most particles in Reaction 1, which is facilitated by the small thickness of the deposit; also, the effective contact between Cu_2O particles and the substrate facilitates electron transfer at the active material-substrate interface. Indeed, this in an advantage of these electrodes, which can deliver acceptable capacity on prolonged cycling without the need for electronic conducting additives. The specific capacity delivered by the cell is lower for thicker electrodes. Thus, Sample E, of greater film thickness, only provided 125 $Ah \cdot kg^{-1}$, which faded to 40 $Ah \cdot kg^{-1}$ after one hundred cycles. However, cell performance was affected not only by film thickness, but also by particle size. The influence of the latter reflected in two

facts. First, although films B and C possessed a similar thickness, the latter, consisting of smaller particles, delivered a higher capacity. Second, the cycling properties of Samples B and D were similar in spite of their differences in thickness, which were small relative to other films (see Table I). Notwithstanding the greater film thickness of Sample D, the deposit was more porous and its grains were smaller and less crystalline, all of which can increase the reactivity of Cu_2O particles towards lithium. These two cells delivered a nearly constant capacity of *ca.* 210 $Ah \cdot kg^{-1}$ upon successive cycling. Our results depart from those reported by Grugeon *et al.*,[6] who found capacity retention on cycling to be strongly dependent on particle size and obtained their best results with micronic particles. We have no irrefutable explanation at present for the little influence of particle size on capacity retention in these films. In any case, our films unarguably exhibit good contact between electrodeposited particles and the substrate.

In summary, the electrodeposition technique is an excellent tool for preparing homogeneous cuprous oxide films with a controlled oxidation state and clean surface. The morphology and thickness of the film can be modulated by adjusting the synthesis conditions. Films thus prepared, particularly those of small or intermediate thicknesses, exhibit a good electrochemical response in lithium cells and excellent coulombic efficiency over repeated charge and discharge cycles.

References

1. P. Poizot, S. Laruelle, S. Grugeon, L. Dupont, and J. M. Tarascon, *Nature (London), 407*, 496 (2000).
2. G. X. Wang, Y. Chen, K. Konstantinov, M. Lindsay, H. K. Liu, and S. X. Dou, *J. Power Sources, 109*, 142 (2002).
3. F. Badway, I. Plitz, S. Grugeon, S. Laruelle, M. Dollé, A. S. Gozdz, and J. M. Tarascon, *Electrochem. Solid-State Lett., 4*, A115 (2002).
4. D. Larcher, M. Masquelier, C. D. Bonnin, Y. Chabre, V. Masson, J. B. Leriche, and J. M. Tarascon, *J. Electrochem. Soc., 150*, A133 (2003).
5. M. N. Obrovac, R. A. Dunlap, R. J. Sanderson, and J. R. Dahn, *J. Electrochem. Soc., 148*, A576 (2001).
6. S. Grugeon, S. Laruelle, S. R. Herrera-Urbina, L. Dupont, P. Poizot, and J. M. Tarascon, *J. Electrochem. Soc., 148*, A285 (2001).
7. Y. Wang and Q. Z. Qin, *J. Electrochem. Soc., 149*, A873 (2002).
8. Y. Wang, Z. W. Fu, and Q. Z. Qin, *Thin Solid Films, 441*, 19 (2003).
9. J. Morales, L. Sánchez, F. Martín, J. R. Ramos-Barrado, and M. Sánchez, *Electrochim. Acta, 49*, 4589 (2004).
10. V. Georgieva and M. Ristov, *Sol. Energy Mater. Sol. Cells, 73*, 67 (2002).
11. E. W. Bohannan, M. G. Shumsky, and J. A. Switzer, *Chem. Mater., 11*, 2289 (1999).
12. M. Winter and J. O. Besenhard, *Electrochim. Acta, 45*, 31 (1999).
13. S. D. Beattie and J. R. Dahn, *J. Electrochem. Soc., 150*, A894 (2003).
14. B. Laik, P. Poizot, and J. M. Tarascon, *J. Electrochem. Soc., 149*, A251 (2002).
15. Y. Zhou and J. A. Switzer, *Scr. Mater., 38*, 1731 (1998).
16. D. Briggs and M. P. Seah, Editors, *Practical Surface Analysis*, 2nd ed., Vol. 1, John Wiley & Sons Ltd, New York (1990).
17. E. Cano, C. L. Torres, and J. M. Bastisdas, *Mater. Corros., 52*, 667 (2001).
18. C. Drouet, C. Laberty, J. L. G. Fierro, P. Alphonse, and A. Rousset, *Int. J. Inorg. Mates., 2*, 419 (2000).
19. A. Débart, L. Dupont, P. Poizot, J.-B. Leriche, and J. M. Tarascon, *J. Electrochem. Soc., 148*, A1266 (2001).